# Correction of Hot Pixel Steps in Aeolus Reprocessed Data

Fabian Weiler, Nafiseh Masoumzadeh and Oliver Reitebuch

*German Aerospace Center (Deutsches Zentrum für Luft- und Raumfahrt e.V., DLR), Institute of Atmospheric Physics, Oberpfaffenhofen 82234, Germany*

## Hot Pixel Issue

- **Hot pixels (HP):** Pixels with enhanced dark current signal in the memory zone of the Mie and Rayleigh Accumulation Charge-Coupled Devices (ACCDs)
- Horizontal features in the wind products **with systematic wind errors of up to several m/s**
- **HP characteristics:**
  - Dark current level changes at random and unpredictable times
  - Different amplitudes
- Mitigation by **regular dark current signal characterization measurements** (**DCMZs**, now 8 per day)
- The **near-real-time (NRT) dark signal correction is imperfect** due to the temporal discontinuity between wind and DCMZ measurements
- HP incuded steps manifest as **sharp steps in the backscatter signal**
- In case a HP changes its level, the dark signal correction is wrong until the next DCMZ is carried out

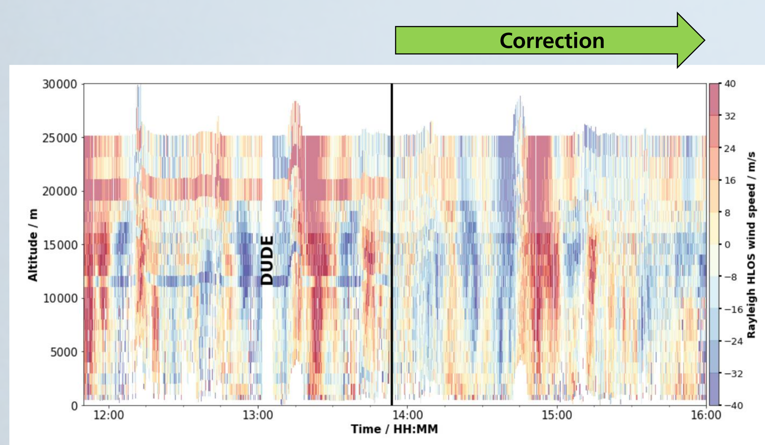


Introduction of the hot pixel correction for the operational Aeolus processing on 14 June 2019. L2B Aeolus Rayleigh-clear HLOS winds before (left to black line) and after the implementation of the DCMZ correction scheme (right to black line).[1]

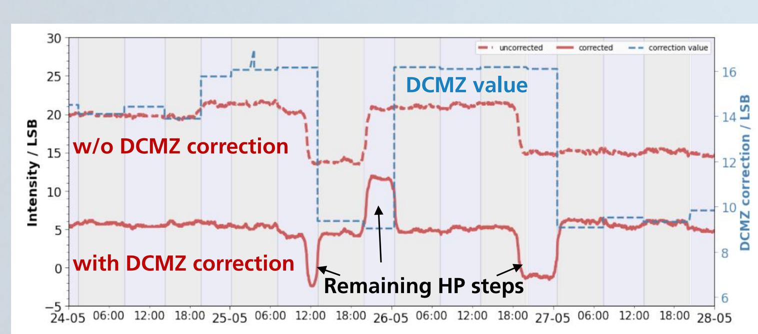


Performance of the NRT DCMZ correction for a Mie hot pixel located in range gate #12 from 24 to 28 May 2020. The solid and dashed red line indicate the signal with and without dark signal correction. The dashed blue line shows the dark signal correction value obtained from four DCMZ measurements per day.

[1] *Weiler, F., Kanitz, T., Wernham, D., Rennie, M., Huber, D., Schillinger, M., Saint-Pe, O., Bell, R., Parrinello, T., and Reitebuch, O.: Characterization of dark current signal measurements of the ACCDs used on board the Aeolus satellite, Atmos. Meas. Tech., 14, 5153–5177, https://doi.org/10.5194/amt-14-5153-2021, 2021.*

## Motivation

- Correction of remaining HP induced signal steps to further mitigate impacts on the data quality
- Due to availability of the complete time series, the **detection of hot pixel induced steps** is easier in the **reprocessing** than in the near-real-time (NRT) processing where only a limited part of the data (one orbit) is available
- Accurate detection of remaining HP steps in the backscatter signal
- Challenge: **Reliable detection** of HP induced steps also in the **presence** of large **atmospheric signal variation** (e.g. for illuminated Rayleigh pixels)
- Development of a time series **change point detection** tool based on **Singular Spectrum Analysis (SSA)**

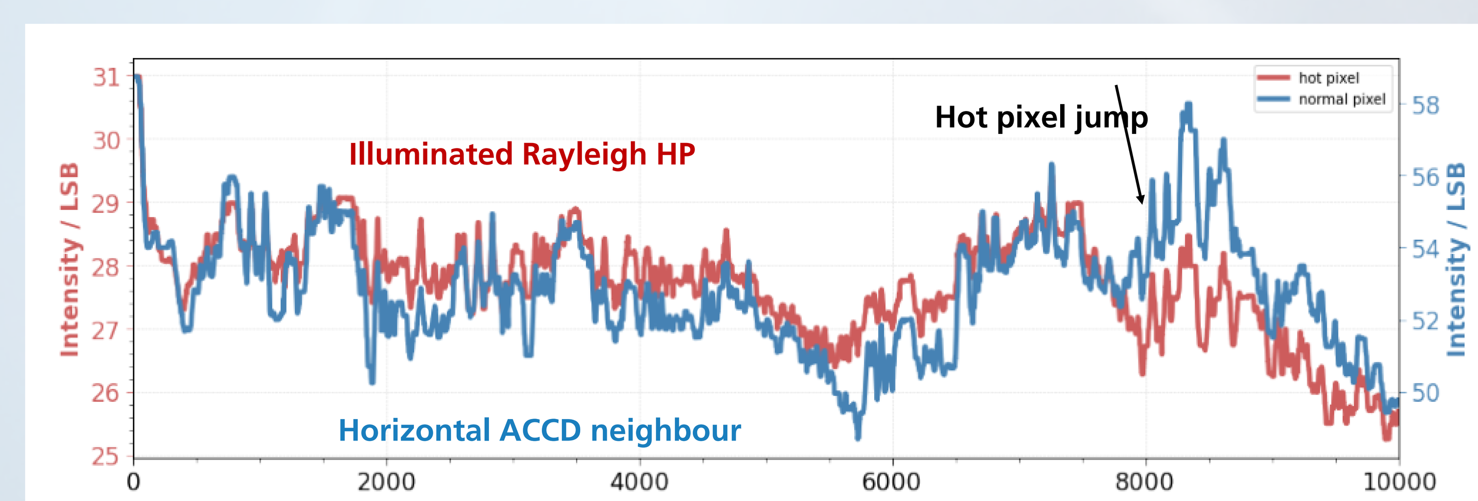


Median-filtered time series (600 obs.) of a Rayleigh hot pixel located in range gate #10 (red) and its right ACCD neighbour (blue) from May 1, 2020 01:03 UTC to May 2, 2020 11:28 UTC.

## Methodology

- Change point detection: „Task of finding time steps where the main characteristics of a time series are changing"
- This problem requires a **unsupervised, non-parametric method** which can be used for **on- and offline** changed point detection → **SSA-based change point detection** suitable candidate
- Basic idea: Application of **Singular Value Decompositon (SVD)** to a matrix representation of the time series
  1. Mapping of a time series to a matrix representation (trajectory matrix) **X**
  2. Application of SVD to **X**
- **Left singular vectors** contain information about the **time series patterns** (mean, periodical components and noise) which can be used to detect change points
- SSA-based methods can easily be extended to **multivariate time series** (d>1) which has the advantage of analysing two neighbouring ACCD pixels at the same time

$$X_d = (x_1^d, x_2^d, \ldots, x_n^d) \Rightarrow \mathbf{X} = \begin{pmatrix} x_1 & x_2 & x_3 & \cdots & x_L \\ x_2 & x_3 & x_4 & \cdots & x_{L+1} \\ x_3 & x_4 & x_5 & \cdots & x_{L+2} \\ \vdots & \vdots & \vdots & \ddots & \vdots \\ x_K & x_{K+1} & x_{K+2} & \cdots & x_n \end{pmatrix}$$

Windows of length K

Mapping of a d-dimensional time series $X_d$ to its trajectory matrix $\boldsymbol{X}^{KxL}$.

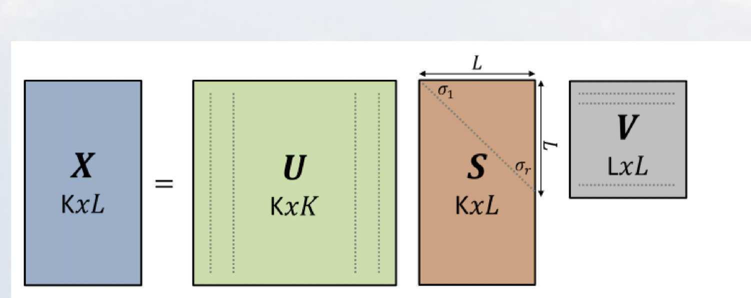


Singular Value Decomposition (SVD) of a matrix $\boldsymbol{X}^{KxL}$ intro three matrices $\boldsymbol{U}^{KxK}$, $\boldsymbol{S}^{KxL}$ and $\boldsymbol{V}^{LxL}$

## Change Point Detection Algorithm

- Two **moving trajectory matrices** $\boldsymbol{H_1}$ and $\boldsymbol{H_2}$ are slided along the time series
- At each time step, $\boldsymbol{H_1}$ and $\boldsymbol{H_2}$ are decomposed using SVD
- A **distance measure** based on the dissimilarity between the left singular vectors $U$ of $\boldsymbol{H_1}$ and $\boldsymbol{H_2}$ is calculated for each time step
- **Large distances** between **both left singular vectors** indicate a structural change in the timeseries, i.e. a **change point**.

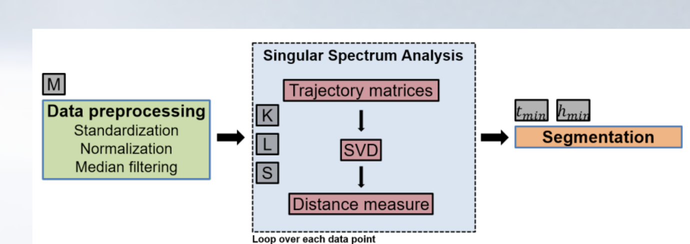


A schematic showing the basic steps of the change point detection algorithm: preprocessing, SSA, and time series segmentation. The grey boxes indicate the configurable parameters of the algorithm.

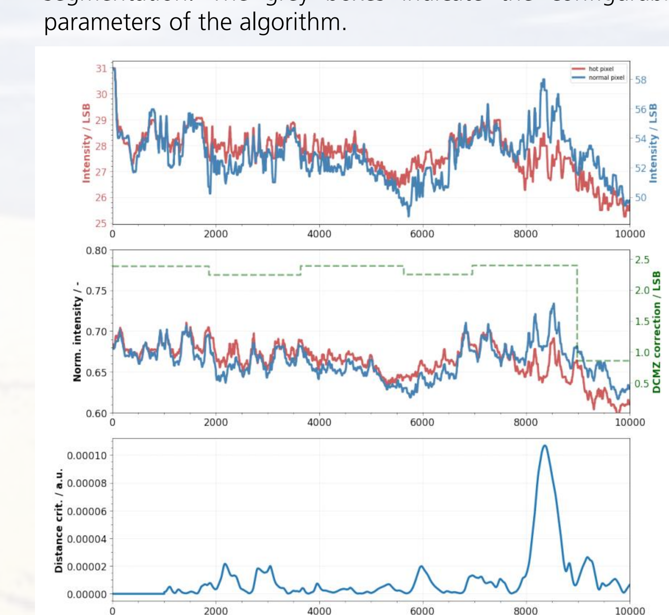


(Top): Median-filtered time series (600 obs.) of a Rayleigh hot pixel located in range gate #10 (red) and its right ACCD neighbour (blue) from May 1, 2020 01:03 UTC to May 2, 2020 11:28 UTC. (Middle): Minimum-maximum scaled signals time series and the DCMZ correction value (green). (Bottom): Distance measure obtained from the change point detection algorithm.

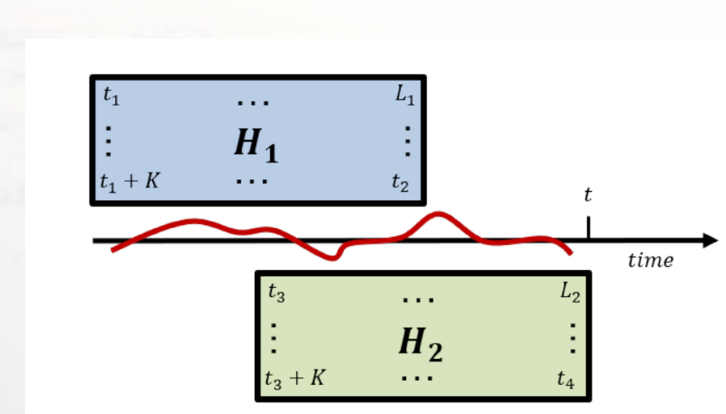


A schematic schowing the principles of the SSA change point detection algorithm with two moving trajectory matrices $\boldsymbol{H_1}$ and $\boldsymbol{H_2}$ evaluated at each time step t of the time series shown in red.

## Optimisation and Validation

- Algorithm has several **tuneable parameters**:
  - Size of the trajectory matrices
  - Median filter size in the preprocessing
- **Optimisation approach** with tailored target function favouring **sharp peaks** in the distance criterion

→ **Optimum set of parameters** for the **Aeolus** hot pixel detection

- Validation:
  - Hot pixel steps labelled for one month of data („ground truth")
  - **93 % precision, 91 % recall**

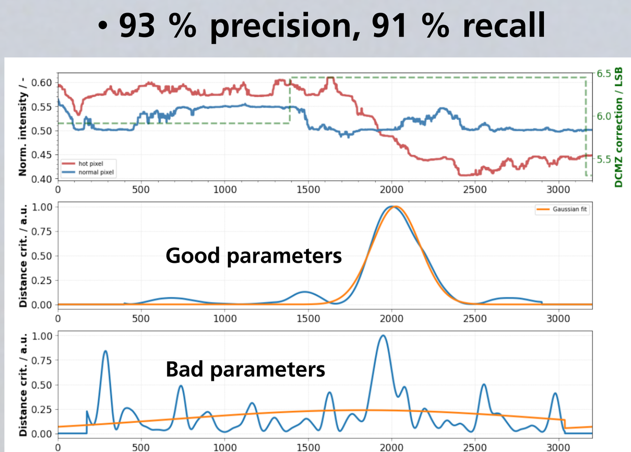


(Top): Median-filtered time series of a Rayleigh hot pixel (600 obs.) located in range gate #10 (red) and its right ACCD neighbour (blue). (Middle) and (Bottom): Distance measure obtained using different sets of algorithm parameters.

## Application to Reprocessing

- First step: **Detection of hot pixel induced steps** in Aeolus L1A **backscatter signals**
- Transfer information about detected change points to the reprocessing chain
- In case a hot pixel induced jump is detected by the algorithm, an **artificial DCMZ measurement** is **created**
- The artificial DCMZ is a copy of the closest nominal DCMZ measurement where only the dark current value of the affected hot pixel is modified
- The artificial DCMZ is valid for the closest orbit start or stop depending on the location of the hot pixel step within the orbit

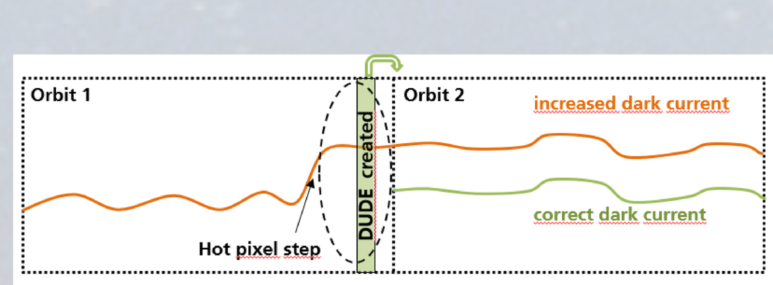


A schematic schowing the principles of the creation of artificial DCMZ measurements to mitigate hot pixel induced steps in the Aeolus reprocessing.

## Reprocessing Results for 08/2018 – 06/2019

- The change point detection algorithm allows for a proper **correction of hot pixel induced steps** in periods with a **low frequency of DCMZ measurements**, e.g. the beginning of FM-A
- The **developed algorithm** was **used** for the first time for the **FM-A** (08/2018 – 06/2019) **reprocessing** (public data release autumn 2022)
- All together **605 artificial DCMZ** files were created to **mitigate hot pixel induced steps arising from 14 hot pixels**

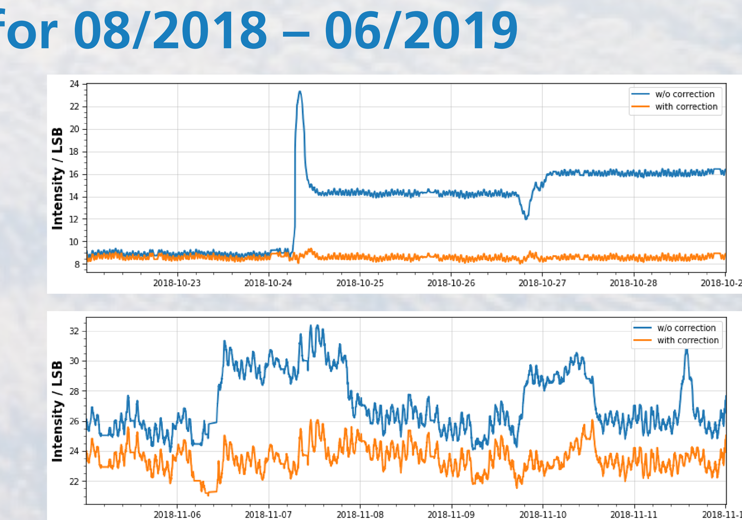


(Median-filtered time series of a Mie hot pixel (400 obs.) located in range gate #1 (top) and a Rayleigh hot pixel located in range gate #10 (bottom) before (blue) and after DCMZ correction (orange) during FM-A.

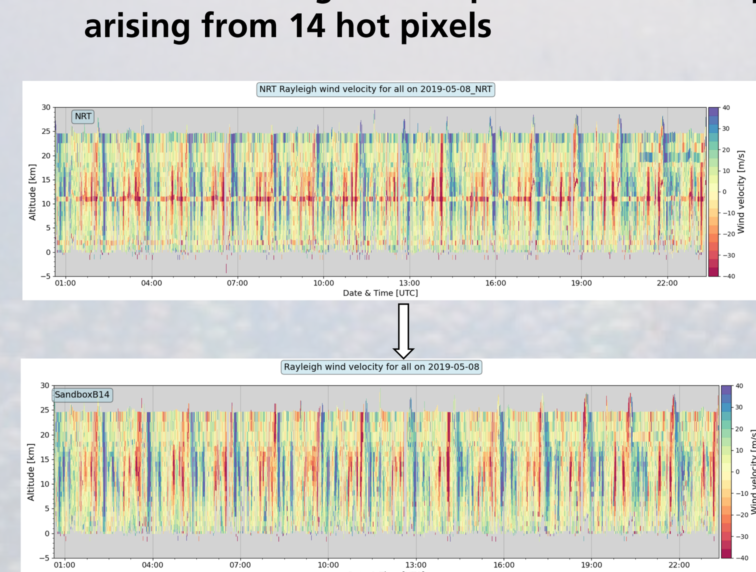

Comparison of L1B Rayleigh HLOS winds of NRT-baseline 2 (top) with reprocessing baseline B14 (bottom) for May 8, 2019.

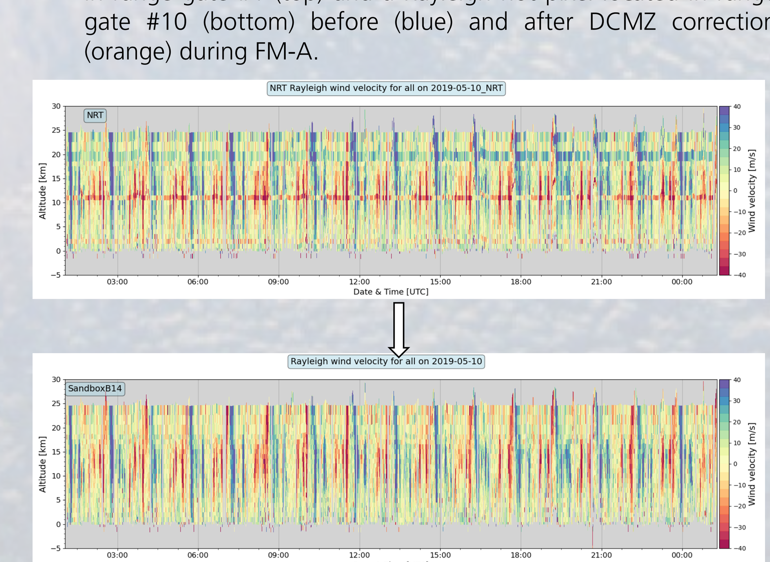

Comparison of L1B Rayleigh HLOS winds of NRT-baseline 2 (top) with reprocessing baseline B14 (bottom) for May 10 2019.